On the Impact of Stochastic Loads and Wind Generation on Under Load Tap Changers

M. A. A. Murad, *Student Member, IEEE*, F. M. Mele, *Student Member, IEEE*, F. Milano, *Fellow, IEEE*
School of Electrical & Electronic Engineering, University College Dublin, Ireland
mohammed.murad@ucdconnect.ie, francesca.mele@ucdconnect.ie, federico.milano@ucd.ie

***Abstract*—This paper compares different models and implementations of the controllers of Under Load Tap Changers (ULTCs) and the impact on such models due to stochastic variations of load power consumption and wind power generation. The main goal of this paper is to show the response of different implementations of the tap changer control to uncertainty and volatility, emphasizing the need of time domain analysis and precise modeling. The case study considers a reduced Irish medium voltage distribution network fed by an ULTC with and without the inclusion of a local wind power plant.**

***Index Terms*—Under Load Tap Changer (ULTC), stochastic modeling, dead band, time delay, voltage control.**

I. Introduction

A. Motivation

As the integration of stochastic distributed renewable energy resources increases, undesirable voltage fluctuations are observed in different levels of power systems. Figure 1 shows a real-world example of this situation. The figure depicts the voltage magnitude at a 110 kV bus level during a day in April 2017 with a sampling time of 0.1 s. The load and the wind generation connected at the distribution system fed by the 110 kV bus lead to frequent tap changing operations of the ULTC. While this behavior is expected, properly reproduce the precise dynamic behavior of ULTC regulators through simulations is not a trivial task. Depending on the model of the ULTCs, tap changing operations can be significantly different. This paper addresses this modeling issue of ULTC from a dynamic point of view, considering stochastic variation of the load power consumption and wind power generation at the distribution system level.

B. Literature Review

Most transformers in distribution networks have under load tap changing capability. The modeling of such ULTCs is crucial for voltage stability analysis [1] due to the presence of non-linearity (dead band, time delay, discrete tap positions) in these transformers. Even though the circuit model of ULTCs is well known, the model of the control of such devices differs depending on the applications and/or implementations [2].

The effect of stochastic distributed generation such as wind power and photo-voltaic on the frequency of tap change and performance of the ULTCs have been studied in [3], [4], [5]. These studies are relevant from the economic point of view as 50% of maintenance cost of such transformers is related to the number of tap operations [6]. However, the aforementioned studies are based on step-wise power flow solutions, and do not consider the dynamic behavior of ULTC controllers. Studies based on time domain or quasi-steady-state simulations are considered in [7] and [8], respectively. These references do not consider stochastic modeling.

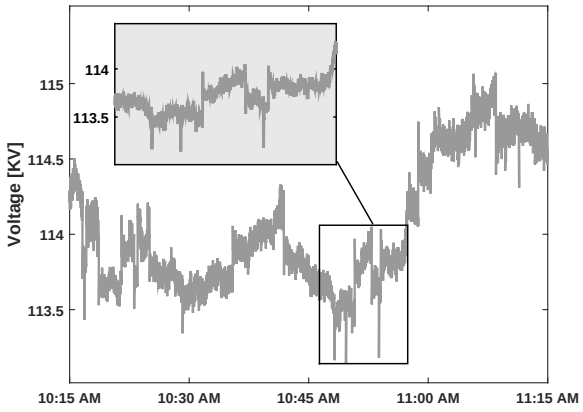

Fig. 1: Voltage at a 110 kV bus in a real system. The measuremnts show stochastic fluctuations due to stochastic renewable energy generation and tap changer.

C. Contributions

Most of the previous studies showed the behavior of ULTC transformers considering either steady-state power flow or quasi steady-state analyses. This is adequate enough for the appraisal of power system operation. However, when considering a short period, e.g., within a time frame of 5 to 15 minutes, stochastic fluctuations due to loads and distributed generation can lead to variations of the tap changers that might not be captured using a steady-state or quasi-steady state approaches. That is why the focus of this paper is on ULTC operations occurring in a time scale of 15 minutes. The main contribution of the paper is that it shows the impact on ULTC tap operation of different control models using stochastic load and wind model performing dynamic simulations.

D. Organization

The remainder of this paper is organized as follows. Section II provides a brief overview of the ULTC transformer and discusses three different control models. Section III presents the stochastic model of the load power consumption and wind

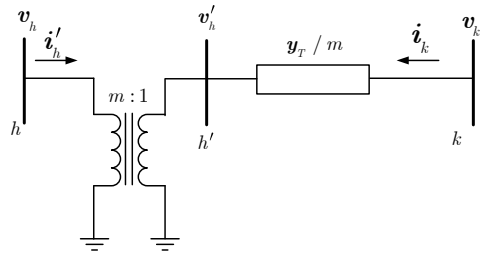

Fig. 2: Equivalent circuit of the transformer with tap ratio module and series impedance.

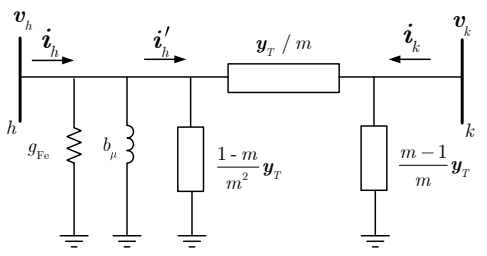

Fig. 3: Equivalent circuit of transformer.

power generation. The dynamic performance of each ULTC control model is compared in the case study presented in Section IV, using a reduced Irish medium voltage distribution network. Finally, in Section V, conclusions and future work directions are drawn.

II. Models of the Under Load Tap Changer

An ULTC is able to control the voltage or the reactive power at the primary or secondary winding of the transformer by varying its tap ratio [9]. This section briefly outlines the ULTC circuit as well as three ULTC control models widely utilized in the literature.

A. Circuit Model

Figure 2 shows the equivalent circuit of a two-winding transformer assuming the tap is on the primary [9]. As $\boldsymbol{v}'_h = \boldsymbol{v}_h/m$, the currents injections at buses h' and k are:

$$\begin{bmatrix} \boldsymbol{i}'_h \\ \boldsymbol{i}_k \end{bmatrix} = \boldsymbol{y}_T \begin{bmatrix} \frac{1}{m^2} & -\frac{1}{m} \\ -\frac{1}{m} & 1 \end{bmatrix} \begin{bmatrix} \boldsymbol{v}_h \\ \boldsymbol{v}_k \end{bmatrix} , \tag{1}$$

where bold face indicate complex numbers. Considering the physical buses h and k and including magnetization and iron losses on the primary winding (see Fig. 3), one obtains:

$$\begin{bmatrix} \boldsymbol{i}_h \\ \boldsymbol{i}_k \end{bmatrix} = \begin{bmatrix} g_{\text{Fe}} + jb_\mu + \boldsymbol{y}_T \frac{1}{m^2} & -\boldsymbol{y}_T \frac{1}{m} \\ -\boldsymbol{y}_T \frac{1}{m} & \boldsymbol{y}_T \end{bmatrix} \begin{bmatrix} \boldsymbol{v}_h \\ \boldsymbol{v}_k \end{bmatrix} , \tag{2}$$

where $\boldsymbol{y}_T = (r_T + jx_T)^{-1}$; g_{Fe}, b_μ, r_T and x_T are transformer iron loss, magnetizing susceptance, resistance and reactance respectively. Finally, the power injections are at buses h and k as follows:

$$\begin{aligned} p_h &= v_h^2(g_{\text{Fe}} + g_T/m^2) - v_h v_k(g_T \cos\,\theta_{hk} + b_T \sin\,\theta_{hk})/m \\ q_h &= -v_h^2(b_\mu + b_T/m^2) - v_h v_k(g_T \sin\,\theta_{hk} - b_T \cos\,\theta_{hk})/m \\ p_k &= v_k^2 g_T - v_h v_k(g_T \cos\,\theta_{hk} - b_T \sin\,\theta_{hk})/m \\ q_k &= -v_k^2 b_T + v_h v_k(g_T \sin\,\theta_{hk} + b_T \cos\,\theta_{hk})/m \ . \end{aligned} \tag{3}$$

B. Control Models

The main elements that compose a ULTC controller are: the measurement of the voltage (or reactive power) on the controlled winding; a dead band, that reduces the sensitivity of the controller; a time delay that limits the number of variations of the tap position; a switching logic that decides whether the tap position has to be changed; and a mechanical actuator that moves the tap. In principle, all these elements should be properly modeled. In the literature, however, mostly only simplified models are considered.

TABLE I: List of ULTC control models

Model	Description	Equations
ULTC 1	Continuous control model	(4)
ULTC 2	Discrete control model	(5)-(8)
ULTC 3	Discrete control model with variable time delay	(5)-(9)

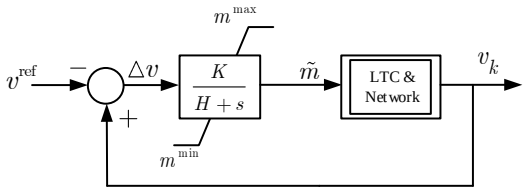

Fig. 4: Continuous model of the ULTC voltage control.

In this subsection, three commonly used control models are considered, namely, (i) continuous model, (ii) discrete model and (iii) discrete model with variable time delay (see Table I).

1) Continuous control model: The continuous control model approximates the tap ratio step Δm to be small, so that tap ratio m can vary continuously [10], as shown in Fig. 4 [9]. The time delay and mechanical actuator are approximated as a lag transfer function and the tap ratio differential equation is given by:

$$\dot{m} = -Hm + K(v_k - v_{\text{ref}}) , \tag{4}$$

where, H, K, v_k and v_{ref} are the integral deviation, inverse time constant, secondary bus voltage and controlled reference voltage, respectively. The dead band is not included in this model.

2) Discrete control model: In this model, the tap ratio is a discrete variable, which can take fixed values in the range of $m^{\max}$ and $m^{\min}$ by a fixed step Δm. The tap can move up or down by one step Δm if the controlled voltage v_k deviates

more than a given dead band db with respect to the reference voltage v^{ref} for longer than a time delay. The model considered here is as follows [2], [11]:

$$e(\Delta v(t), m(t-\Delta t), db, m^{\max}, m^{\min}) = \begin{cases} 1, & \text{if } \Delta v(t) > db \text{ and } m(t-\Delta t) < m^{\max} \\ -1, & \text{if } \Delta v(t) < -db \text{ and } m(t-\Delta t) > m^{\min} \\ 0, & \text{otherwise ,} \end{cases} \quad (5)$$

$$c(e(t), c(t-\Delta t)) = \begin{cases} c(t-\Delta t) + \Delta t, & \text{if } e(t) = 1 \text{ and } c(t-\Delta t) \geq 0 \\ c(t-\Delta t) - \Delta t, & \text{if } e(t) = -1 \text{ and } c(t-\Delta t) \leq 0 \\ 0, & \text{otherwise ,} \end{cases} \quad (6)$$

$$f(e(t), c(t), \tau(t)) = \begin{cases} 1, & \text{if } e(t) = 1 \text{ and } c(t) > \tau(t) \\ -1, & \text{if } e(t) = -1 \text{ and } c(t) < \tau(t) \\ 0, & \text{otherwise ,} \end{cases} \quad (7)$$

where e models the dead band, f the time delay, c is a memory function that stores the time elapsed since the tap change, t is the current simulation time, $t - \Delta t$ is the previous simulation step and $\tau(t) = \tau_0$ is the constant time delay. Finally, the tap ratio is switched as follows:

$$m(t) = m(t-\Delta t) + f(e(t), c(t), \tau(t))\Delta m \ . \quad (8)$$

3) Discrete control model with variable delay: This model differs from the discrete control model above in such way, that it considers a variable time delay. The higher the voltage error Δv the faster the tap change [2], [12] will be. The time delay is given by the following expression:

$$\tau(t) = \begin{cases} \tau_0 \frac{db}{|\Delta v|}, & \text{if } |\Delta v| > db \\ \tau_0, & \text{otherwise .} \end{cases} \quad (9)$$

III. Stochastic Models

This section outlines the load consumption and wind speed models considered in this study. These include stochastic perturbations modeled by means of the following Itô-type differential equation:

$$dx(t) = a(x(t), t)dt + b(x(t), t)dw(t), \quad (10)$$

where $x(t)$ is the variable affected by noise, $a(x(t), t)$ and $b(x(t), t)$ are the drift and the diffusion terms respectively, and $w(t)$ is a standard Wiener process [13]. Equation (10) is a general expression that can take into account both Gaussian and non-Gaussian processes and is thus appropriate to model load power variations [14] and wind speed fluctuations [15].

A. Stochastic Voltage Dependent Load Model

The well-known Voltage Dependent Load (VDL) model is given by [9]:

$$\begin{aligned} p_L(t) &= -p_{L0}(v(t)/v_0)^\gamma \\ q_L(t) &= -q_{L0}(v(t)/v_0)^\gamma, \end{aligned} \quad (11)$$

where p_{L0} and q_{L0} are the active and reactive powers at the the nominal voltage v_0; $v(t)$ is the voltage magnitude of the bus where the load is connected; and γ is the power exponent.

Merging together the stochastic equation (10) and the load equations (11) lead to a Stochastic VDL (SVDL) load model. Since load variations are approximately Gaussian and show a constant standard deviation, we define the diffusion terms $a(\cdot)$ and $b(\cdot)$ in (10) to resemble an Ornstein-Uhlenbeck process [14]. The resulting SVDL load model is:

$$\begin{aligned} p_L(t) &= (-p_{L0} + \eta_p(t))(v(t)/v_0)^\gamma \\ q_L(t) &= (-q_{L0} + \eta_q(t))(v(t)/v_0)^\gamma \\ \dot{\eta}_p(t) &= \alpha_p(\mu_p - \eta_p(t)) + b_p\xi_p \\ \dot{\eta}_q(t) &= \alpha_q(\mu_q - \eta_q(t)) + b_q\xi_q, \end{aligned} \quad (12)$$

where the α terms are the speed at which the stochastic variables η are "attracted" towards the mean values μ, and the b terms represents the volatility of the processes.

B. Stochastic Wind Model

To emulate the wind speed, $a(\cdot)$ and $b(\cdot)$ in (10) must be defined so that the probability distribution of $x(t)$ is a Weibull process. It is also important to reproduce the autocorrelation of the wind speed, which, in this paper, is assumed to be exponentially decaying. This can be achieved through the regression theorem and the stationary Fokker-Planck equation, as thoroughly discussed in [15]. The resulting drift and diffusion terms are:

$$\begin{aligned} a(x(t)) &= -\alpha \cdot (x(t) - \mu_{\text{W}}) \\ b(x(t)) &= \sqrt{b_1(x(t)) \cdot b_2(x(t))} \ , \end{aligned} \quad (13)$$

where α is the autocorrelation coefficient; μ_{W} is the mean of the Weibull distribution; and

$$b_1(x(t)) = \frac{2 \cdot \alpha}{p_{\text{W}}(x(t))}$$

$$b_2(x(t)) = \lambda \cdot \Gamma\left(1 + \frac{1}{k}, \left(\frac{x(t)}{\lambda}\right)^k\right) - \mu_{\text{W}} \cdot e^{-(x(t)/\lambda)^k} \ ,$$

where $p_W(\cdot)$ is the Weibull Probability Density Function (PDF); $\Gamma(\cdot, \cdot)$ is the incomplete Gamma function; k and λ are the shape and scale parameters of the Weibull distribution, respectively.

IV. Case Study

A real-world distribution network is used in this section to study the dynamic behavior of the three ULTC control configurations described in Section II. All simulations results discussed in this section have been obtained with the Python-based software Dome [16].

A. Test System

The test network used is a small Irish distribution system with both radial and meshed configurations [17]. The network includes eight buses, six loads, one wind generation, one slack bus and eight transmission lines. The operating nominal voltage of B1-B8 is 38 kV and the buses are fed by an ULTC

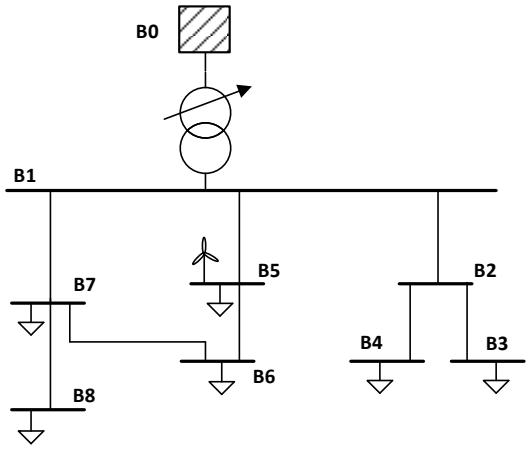

Fig. 5: Topology of the test distribution network [17].

TABLE II: ULTC parameters

Name	Values
ULTC 1	$H = 0.001$, $K = 0.1$
ULTC 2, 3	$db = 2\%$, $\tau_0 = 30$ s, $\Delta m = 0.0125$
All models	$m^{\max} = 1.2$, $m^{\min} = 0.8$

type step down transformer from a 110 kV network. The network topology is shown in Fig. 5. Network parameters can be found in [17].

B. Simulation Results

The active and reactive power loading of the test system are 15.02 MW and 8.29 MVAr respectively and the nominal wind farm capacity is 12 MW. 10% of the loads is a SVDL modeled as in (12) and the 90% is modeled as constant PQ ($\gamma = 0$ in (12)). The wind generator model is a 5th-order doubly-fed induction generator with variable-speed wind turbine having discrete pitch control, first-order automatic voltage regulator, algebraic turbine governor and Maximum Power Point Tracking (MPPT). The input to wind turbine is a stochastic wind modeled as in (13). The parameters utilized for the three ULTC models are given in Table II. 500 15-minute Monte Carlo simulations are considered for each model and parameter set.

Figures 6 to 8 show the trajectories of voltage at bus 1 for the 500 simulations considering three ULTC types. Figures 6-8 also include the mean, μ, and $\mu \pm 3\sigma$, where σ is the standard deviation. The mean and the standard deviation of the 500 trajectories are calculated at every time instant of the simulation interval which is 0.01 s. The results obtained for ULTC 1 (continuous model) is used as reference case. The continuous control provide by ULTC 1, in fact, can be assumed to be the *optimum* with which the performance of the discrete models can be compared.

The mean values of voltage at bus 1 at every time instant for 500 trajectories using ULTC 2 and ULTC 3 also shown in Fig. 9. The difference in the means and standard deviations

TABLE III: Average number of ULTC tap operations

Parameters	ULTC 2	ULTC 3
db = 2 %, τ_0 = 30 s	1.008	12.73
db = 3 %, τ_0 = 30 s	0.236	9.157
db = 4 %, τ_0 = 30 s	0.116	6.578
db = 2 %, τ_0 = 60 s	0.904	6.60
db = 2 %, τ_0 = 120 s	0.744	3.29

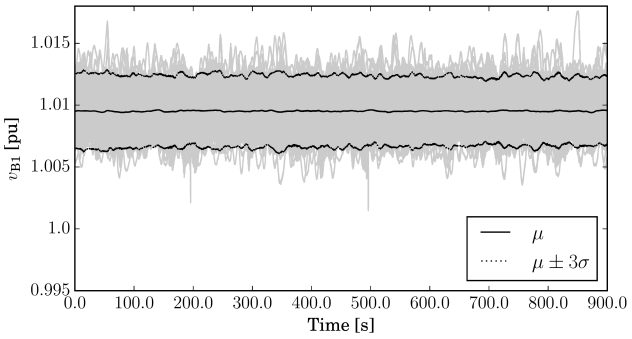

Fig. 6: 500 stochastic trajectories and statistical properties of the bus 1 voltage using ULTC 1.

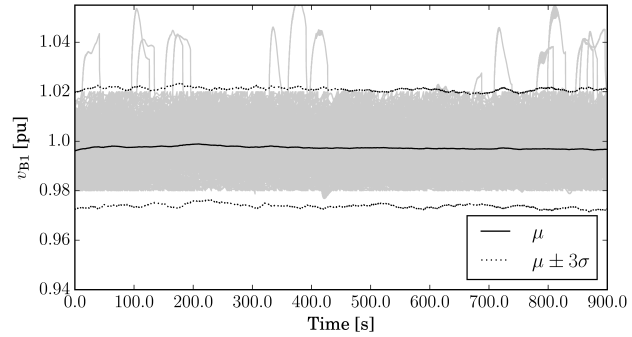

Fig. 7: 500 stochastic trajectories and statistical properties of the bus 1 voltage using ULTC 2.

achieved using ULTC 2 and ULTC 3 are insignificant. However, the number of tap operations using ULTC 3 is notably higher than ULTC 2 for the same dead band and time delay settings, as illustrated in Table III. To choose appropriate values for the time delay and dead band these references are used [18], [19]. As expected, the higher the time delay and dead band, the lower the number of tap changes; however using a higher dead band and delay can deteriorate the voltage response. For all settings of dead band and time delay, ULTC 3 results in higher number of tap changes than ULTC 2.

Finally, for completeness, the test network is simulated with no wind generation using ULTC 2 ($db = 2\%$ and $\tau_0 = 30$ s) and SVDL. Figure 10 shows 500 stochastic trajectories and statistical properties of the voltage variations of the bus 1. The average number of tap operations (0.004) are much smaller than those obtained in the scenario with wind generation.

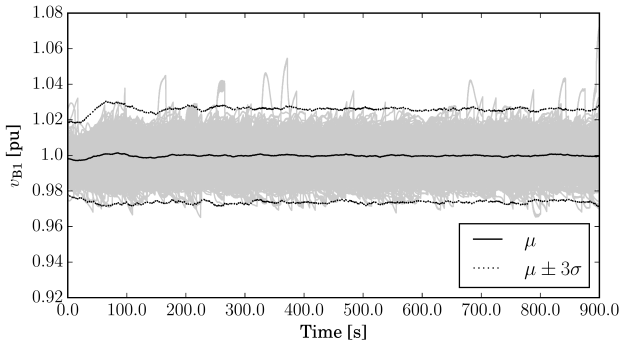

Fig. 8: 500 stochastic trajectories and statistical properties of the bus 1 voltage using ULTC 3.

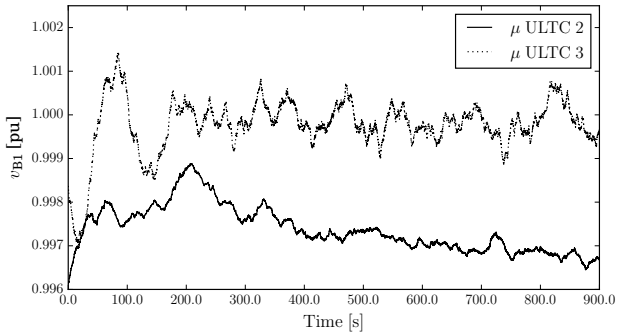

Fig. 9: Average voltage trajectory of bus 1 using ULTC 2 and 3.

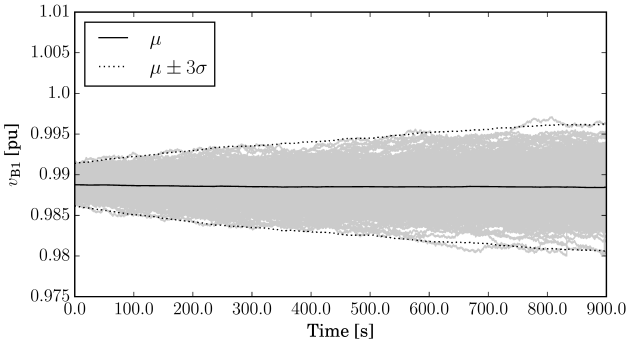

Fig. 10: 500 stochastic trajectories and statistical properties of the bus 1 voltage using ULTC 2 for no wind power generation.

V. Conclusions

The paper discusses the dynamic performance of different models of ULTC transformers in distribution networks with inclusion of stochastic loads and wind generation. A first conclusion of the paper is that, when considering stochastic processes, the time domain analysis is necessary to account for ULTC tap variations that happens in the time scales of minutes as these cannot be properly captured considering only a steady-state or quasi-steady-state analysis. Simulation results also allow concluding that, depending on the ULTC control model, the number of tap operation can be significantly different, so it is important to accurately implement the control logic. This is another aspect that cannot be fully captured by conventional steady-state analyses. Future work will consider larger distribution networks and consider more detailed ULTC model.

Acknowledgment

Mohammed Ahsan Adib Murad and Federico Milano are supported by Science Foundation Ireland (SFI) under Grant No. SFI/15/IA/3074. Federico Milano is also a beneficiary of the EC Marie Skłodowska-Curie CIG No. PCIG14-GA-2013-630811.

References

[1] P. Kundur et al., "Definition and Classification of Power System Stability IEEE/CIGRE Joint Task Force on Stability Terms and Definitions," *IEEE Transactions on Power Systems*, vol. 19, no. 3, pp. 1387-1401, Aug. 2004.

[2] F. Milano, "Hybrid Control Model of Under Load Tap Changers," *IEEE Transactions on Power Delivery*, vol. 26, no. 4, pp. 2837-2844, Oct. 2011.

[3] S. N. Salih, P. Chen, O. Carlson, "The Effect of Wind Power Integration on the Frequency of Tap Changes of a Substation Transformer," *IEEE Transactions on Power Systems,* vol. 28, no. 4, pp. 4320-4327, Nov. 2013.

[4] S. S. Baghsorkhi, I. A. Hiskens, "Impact of Wind Power Variability on Sub-Transmission Networks," *IEEE Power & Energy Society General Meeting,* San Diego, CA, 2012, pp. 1-7.

[5] C. Long, A. T. Procopiou, L. F. Ochoa, G. Bryson, D. Randles, "Performance of OLTC-based Control Strategies for LV Networks with Photovoltaics," *IEEE PES General Meeting,* Denver, CO, pp. 1-5, July 2015.

[6] James O'Donnell, "Voltage Management of Networks with Distributed Generation," PhD Thesis, The University of Edinburgh, 2007.

[7] D. Ranamuka, A. P. Agalgaonkar, K. M. Muttaqi, "Examining the Interactions between DG Units and Voltage Regulating Devices for Effective Voltage Control in Distribution Systems," *IEEE Transactions on Industry Applications,,* vol. 53, no. 2, pp. 1485-1496, Mar.-Apr. 2017.

[8] G. K. Ari, Y. Baghzouz, "Impact of High PV Penetration on Voltage Regulation in Electrical Distribution Systems," *International Conference on Clean Electrical Power (ICCEP),* Ischia, pp. 744-748, June 2011.

[9] F. Milano, *Power System Modelling and Scripting,* London: Springer, 2010.

[10] Q. Wu, D. H. Popovic, D. J. Hill, M. Larsson, "Tap Changing Dynamic Models for Power System Voltage Behaviour Analysis," *Power Systems Computation Conference (PSCC),* Trondheim, Norway, 1999.

[11] J. H. Choi and S. I. Moon, "The Dead Band Control of LTC Transformer at Distribution Substation," *in IEEE Transactions on Power Systems,* vol. 24, no. 1, pp. 319-326, Feb. 2009.

[12] Q. Wu, D.H. Popović, D.J. Hill, "Avoiding Sustained Oscillations in Power Systems with Tap Changing Transformers," *International Journal of Electrical Power & Energy Systems*, vol. 22, no. 8, pp. 597-605, 2000.

[13] C. Gardiner, *Stochastic Methods: A Handbook for the Natural and Social Sciences, 4th ed.,* New York, NY: Springer-Verlag, 2009.

[14] F. Milano, R. Zárate-Miñano, "A Systematic Method to Model Power Systems as Stochastic Differential Algebraic Equations," *IEEE Transactions on Power Systems,* vol. 28, no. 4, pp. 4537-4544, Nov. 2013.

[15] R. Zárate-Miñano, F. M. Mele, F. Milano, "SDE-based Wind Speed Models with Weibull Distribution and Exponential Autocorrelation," *IEEE PES General Meeting*, Boston, MA, pp. 1-5, July 2016.

[16] F. Milano, "A Python-Based Software Tool For Power System Analysis," *IEEE PES General Meeting*, Vancouver, BC, pp. 1-5, July 2013.

[17] C. Murphy, A. Keane, "Local and Remote Estimations Using Fitted Polynomials in Distribution Systems," *IEEE Transactions on Power Systems*, vol. 32, no. 4, pp. 3185-3194, July 2017.

[18] M. Larsson, "Coordinated Voltage Control in Electric Power Systems," PhD Thesis, Lund University, Sweden, 2007.

[19] Technical Report PES-TR19, "Test Systems for Voltage Stability Analysis and Security Assessment," *IEEE Power and Energy Society*, Aug. 2015.